Interfacial leakage of elastomer seals at low temperatures

A. G. Akulichev[a], A. T. Echtermeyer[a], B. N. J. Persson[b,c]

[a]*Department of Mechanical and Industrial Engineering (MTP), Norwegian University of Science and Technology, Richard Birkelandsvei 2B, N-7491 Trondheim, Norway*
[b]*PGI-1, FZ Jülich, Germany, EU*
[c]*www.MultiscaleConsulting.com*

Abstract

Interfacial leakage of air in hydrogenated nitrile butadiene rubber (HNBR) O-ring seals exposed to sub-ambient temperatures is studied. Flange-type fixtures with sealing surfaces produced by 3 different surface finish processes are used. When the seals are cooled down to temperatures below the elastomer glass transition point T_g of (−23 °C), an abrupt increase of air leakage ($> 10^{-2}$ cm^3/min) is observed. The effects of surface finish conditions, compression ratio, grease lubrication and additions of carbon black in the HNBR on the cold leakage are discussed. Persson's contact mechanics and effective medium leakage theory coupled with finite element analysis (FEA) of the HNBR seals are utilized to capture the changes in the contact area and pressure with cooling and predict the seal failure temperatures. The main cause for the cold seal failures is believed to be the detachment of the elastomer seals from their mating sealing parts due to the elastomer thermal contraction and the negligible recovery of the HNBR in cold environment. In addition, the adhesive rubber-substrate interface influences the detachment and seal failure.

Keywords:
Elastomer, Seals, Leakage, Low-Temperature Extreme

1. Introduction

Elastomeric seals are used in almost any industrial pressure retaining equipment operating at low and high pressure, e.g. in oil and gas, automotive or aerospace applications. These seals usually have excellent flexibility, resilience and elastic recovery properties and do not require very fine surface finish to make a good seal, as, for example, thermoplastic seals would demand. There are, however, factors under which the pressure integrity of elastomeric seals can be compromised. One of these influencing factors is exposure to a cold environment which might, in fact, lead to catastrophic consequences, as, for instance, in the Challenger disaster [1].

Among all fluids, sealing of gases represents the most difficult task for engineers due to their extremely low viscosity. The gas leakage in elastomer seals arises from gas permeation through the materials and from the interfacial (or contact) leakage. The permeation of gases through elastomers is known to decrease with temperature reduction [1, 2, 3] and is, thus, not as significant at low temperatures as the interfacial leaks [2]. The Challenger catastrophe triggered scientists and engineers from a variety of industries to study the low-temperature behaviour of elastomer seals to be used in gas containing systems. As a result of their efforts, some publications appeared [4, 5, 6, 7, 8, 9, 10, 11, 12, 13, 14, 15, 16]. A short summary of the experimental details and findings of the existing literature is given in Table 1.

The sealing experiments undertaken in different conditions and using different equipment show some similarities. Thus, the majority of seals failed at temperatures approximately 10-35 °C below T_g depending on their compression level and the exerted pressure difference. Hence, T_g does not accurately define the low-temperature limit of serviceability of elastomeric seals. Furthermore, T_g can be determined by several methods, which in general do not give the same results.

Another interesting observation can be made considering the effect of gas pressure: high (≥ 100 bar) pressure difference, if applied prior to cooling of the sealed joint, might result in lower leakage temperatures [8, 10]. Higher failure temperatures were obtained in low-pressure (< 100 bar) systems [5, 6, 11, 12, 14], or in high-pressure systems pressurized after the cooling step [10]. Furthermore, there are indications that pressure and temperature cycling from

low to high values might yield increased leak temperatures [17], but not much experimental data are available to public for these cases.

Most of the earlier investigators used commercial seals with scarcely reported low-temperature properties of the seal materials (typically only the glass transition T_g and sometimes 10 % retraction TR-10 temperatures) and the sealed surface properties. Therefore, the mechanisms of cold leakage of elastomeric seals have remained unclear, except for the case where the sealing gap was artificially increased and seals failed due to their slow elastic recovery at low temperatures near their T_g [13, 16, 20]. This is, however, an extreme scenario which will not be considered herein. The main objective of this work is to understand the phenomena governing the leakage of static elastomeric seals in flange-type joints at low temperatures. The effects of filler in the elastomer and lubrication will be considered as well. The most common scenario when seals are mounted in a joint at ambient temperature inside a workshop or an assembly site and then brought to a cold service is followed. Prediction of the temperature at which the particular elastomer seal fails is of the most interest and aimed in this work.

Table 1: Short summary of the low-temperature leak test data. The imposed compression and applied gas pressure difference are given in parentheses, the method employed to determine T_g is also given in parentheses where available; for more details the reader is referred to the indicated publications. ΔT indicates the difference between the measured leakage temperature T_{fail} and the glass transition. Special test conditions are explained in notes

Elastomer type	T_g, °C	TR-10, °C	Typical conditions		Special conditions		Notes
			T_{fail}, °C	ΔT, °C	T_{fail}, °C	ΔT, °C	
Taylor [8] (15% compression / 345 bar)							
Nitrile	-37 (DMTA)		-56	-19			
Arctic Nitile	-35 (DMTA)	-49	-62	-27			
Camlast 1049	-18 (DMTA)	-19	-40	-22			
Aflas	7 (DMTA)		-23	-30			
Viton	3 (DMTA)		-34	-37			
Burnay and Nelson [6] (1 bar)							
FKM E60C	-18 [18]		-30	-12			
Stevens et al [5, 18] (10 /20 % compression / 14 bar)							
FKM E60C	-18 [18]		-31	-13			Results are for 10 % compression
FKM B70	-21 [18]		-33	-12			
FKM B600	-13 [18]		-26	-13			
FKM GLT	-29 [18]	-31 [18]	-44	-15			
FKM GLFT	-23 [18]	-24 [18]	-36	-13			
Weise et al [9] (25 % compression / 1 bar)							
Viton1	-7		-35	-28			
Viton2	1		-20	-21			
Viton3	-6		-31	-25			
Viton5	-23		-44	-21			
EPDM	-30		-61	-31			
Silicone	-31		-63	-32			
Warren [10] (16.6-18.5% compression / 100 (175) bar)							
HNBR LT	-32 (DMTA)	-36	-54	-22	-41	-9	Pressurized after the cooling step
FKM LT	-19 (DMTA)	-31	-55	-36	-32 (-40)	-13(-21)	
FKM ULT	-27 (DMTA)	-40	-56	-29	-42(-45)	-15(-18)	
Jaunich [12] (13-38 % compression / 1 bar)							
FKM	-18 (DSC, 10K/min)		-29	-11			13 % compression
			-33	-15			25 % compression
			-53	-35			38 % compression
Omnés and Heuillet [14] (24 % compression / 5 bar)							
HNBR	-18 (DMTA, 1 Hz)				-30	-12	Pressurized after the cooling step
Grelle et al [13] (25 % compression / 1 bar)							
FKM	-17 (DSC, 10K/min)		-38	-21	-10	7	Partial release of compression

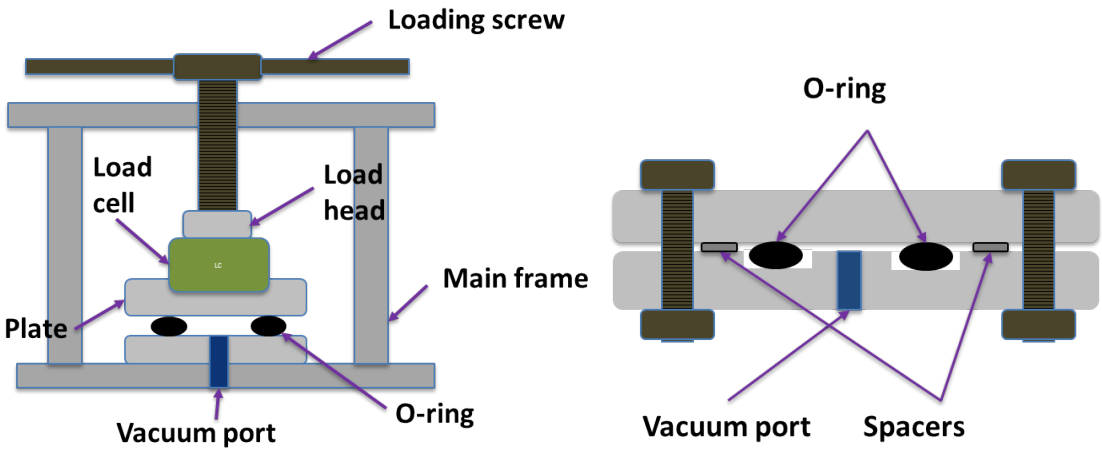

(a) Leak test rig with a load cell.

(b) Leak test flange.

Figure 1: Leak test rigs used in the experiment (schematic).

2. Materials and methods

The cold sealing experiments reported here were performed using a custom-built thermal chamber coupled with heat exchanger piping connected to a recirculating coolant bath manufactured by Julabo. The interiors of the chamber with test rigs can be cooled down to about −52 °C in the experimental set-up.

Two configurations of test rigs were utilized in the experiment. The first one was based on the compression rig concept used in stress relaxation experiments [21] and features compression (sealing) force measurements by a 2.5 kN compression load cell, see Fig. 1a. Pre-defined compression is exerted to an O-ring by a screw in this set-up. The sealing counter-faces have root mean square (RMS) surface roughness of 0.95 µm. The main purpose of the measurements with this rig was to measure the sealing force variation with cooling. Vacuum creates additional compressive force to the seal estimated to be about 800 N leading to lower failure temperatures, especially if the pressure difference is applied at temperatures above the T_g. As a result, another rig was also utilized for measurement of leak rates in cold environment.

The second rig is schematically illustrated in Fig. 1b and represents a simple flange arrangement accommodating an O-ring and exchangeable flange parts having different sealing surface topography as will be described later. A set of spacers was selected to fix the desired seal compression δ. The temperature of the tested O-rings was measured by two thermocouples positioned near the seals; the average values of the thermocouple readings are reported. The sealing surfaces were cleaned with ethanol prior to each test, and the seals were mounted dry at a temperature of 24 ± 1 °C. In addition, several experiments were carried out with application of silicone grease (Molykote 33 Medium).

A vacuum pump connected to the leak port in the test fixtures was used to create a pressure difference between the system and ambient environment. The system (vacuum) pressure and leak rate was continuously measured during each test by a vacuum pressure transducer and supplemented by a flow meter with a resolution of 10^{-3} cm^3/min. The overall system leakage (which includes the leakage in the fittings and air permeation through the polymer parts) was measured to be approximately 2×10^{-3} cm^3/min by the pressure rise method.

Three flange parts with different surface finish were used in the leak measurements. The sealing surfaces were prepared by milling, turning and grinding processes and possess rather different surface roughness. Their surface topography characteristics in the direction orthogonal to the leakage path are summarised in Table 2. The surface roughness of the milled surface finish is somewhat higher than usually specified in engineering documentation, however that was made intentionally to promote leakage. The sealing area topography of the flange parts is depicted in Fig. 2a, while Fig. 2b shows the computed one-dimensional (1D) surface roughness power spectra. It should be noted that the surface roughness is anisotropic in all cases studied here.

Table 2: Surface roughness properties of the sealing surfaces used in the flange experiment. Line scan was performed by stylus profilometer with a lateral resolution of 0.56 µm and track length of 10 mm.

Surface finish	Surface roughness parameters				
	R_a, µm	R_q, µm	R_v, µm	R_p µm	RMS slope
Milling	1.7806	2.1588	-6.189	5.38	0.1807
Turning	0.4081	0.5069	-1.043	1.212	0.0083
Grinding	0.4788	0.6471	-3.812	2.517	0.0928

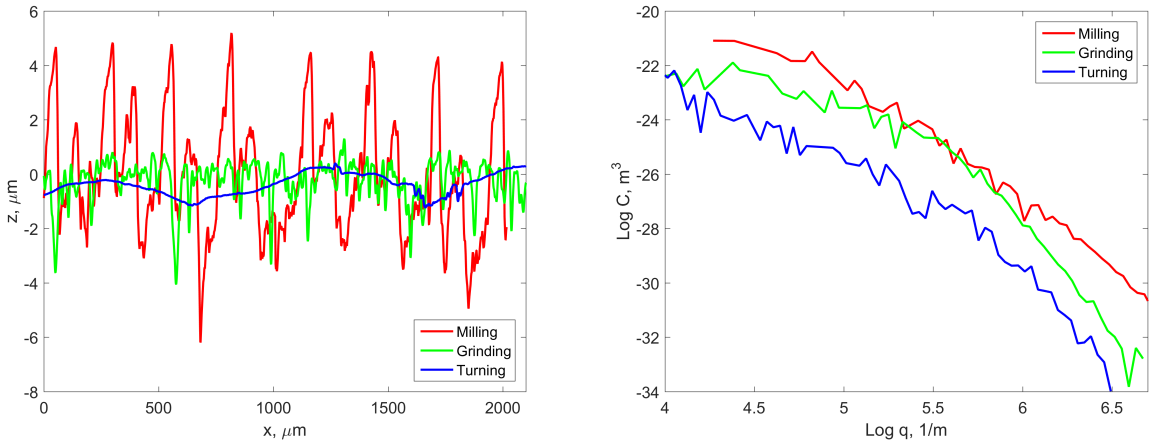

(a) (b)

Figure 2: a) topography measured by stylus profilometer and b) 1D surface roughness power spectra of the indicated sealing surfaces.

For the experiments hydrogenated nitrile butadiene rubber (HNBR) O-rings of ca. 108 mm inner diameter and 5.3-5.5 mm cross section diameter were manufactured in lab environment by compression moulding. Due to the variance in the cross section diameter of the seals, the attained compression levels in flange-type experiment were somewhat different. The basic material is HNBR having 96 % saturated polybutadiene with 36 % acrylonitrile content. Two formulations were used: one with 20.4 Vol.% N-330 HAF carbon black (CB) loading and the other without it (further referred to as unfilled HNBR). The full description of the material composition, the processing details and the material properties were provided in the previous publications [19, 20, 21]. It is important to mention that the elastomers have a T_g of about $-16\,^{\circ}\mathrm{C}$ as determined by dynamic mechanical thermal analysis (DMTA) experiments at the measurement frequency f of 1 Hz [20] or $-23\,^{\circ}\mathrm{C}$ as determined from differential scanning calorimetry (DSC) measurements conducted using a heating rate of $20\,^{\circ}\mathrm{C/min}$ [19].

In the flange-based set-up, three O-rings of each compound were tested against each of three sealing surfaces using three different compression ratios, so the total number of leakage tests was 54. The minimum compression ratio δ used in the experiments was rather low, i.e. $\approx 7-8\,\%$ (a typical engineering practice is to have $\delta \approx 15-30\,\%$). Such low values of seal compression ratio were also needed in order to establish a correlation with the seal failure temperatures. For degrees of compression higher than 30 %, the measurements of seal failures can not be made due to a limited cooling power of the test unit.

3. Results

The leak rates of the studied seals do not change much with cooling to temperatures approximately above $-25\,^{\circ}\mathrm{C}$. At certain temperatures below it an abrupt increase in the air leakage occurs, as for instance depicted in Fig. 3. This finding is in accordance with the cold seal failures experienced in the past works [2, 6, 9, 11, 12]. We refer to the temperature at which the leak rate abruptly increases ($> 10^{-2}\,\mathrm{cm^3/min}$) reflecting the seal failure as leakage temperature. In order to stop such large leaks, the seals have to be heated to temperatures several degrees higher then that at the onset of the large leak (see Fig. 3). The variation of the leakage temperature with O-ring compression is shown in Fig. 4a-4c for all studied counter-surfaces.

The leak data feature a wide distribution of leak temperatures depending on the filler content, the sealing surface topography and the seal compression level. The leak temperature of the seals is found to decrease with increase of O-ring compression for all types of surface finish and regardless of CB content in HNBR. This finding is in agreement with previous observations [9, 12]. The most plausible reason for the reduction of seal failure temperatures with the compression ratio is the increased seal contact width ($L_x = 2a$ where a is the semi-contact width) which yields a larger path for gas molecules to travel through the contact interface as described by Jaunich [12]. Another possible reason for the lower failure temperatures measured in the experiments with highly compressed seals is a much higher contact area, see also Fig. 7a and the analysis part.

The effect of larger seal compression is more pronounced in the CB filled HNBR seals. Furthermore, the seals made of CB filled HNBR in general demonstrate lower leak temperatures as compared to the unfilled HNBR seals. The highest leak temperature (about $-28\,^{\circ}\mathrm{C}$) was observed in the unfilled HNBR seals at $\approx 7\,\%$ compression with the roughest counter-surface, while the lowest leak temperatures below $-45\,^{\circ}\mathrm{C}$ were found in the filled HNBR seals at $\approx 30\,\%$ compression against the most smooth sealing counter-surface in the experiment.

The variation of the leak temperatures with the surface finish conditions is illustrated in Fig. 5a and Fig. 5b for unfilled and filled HNBR respectively. The positive effect of a smoother sealing surface on the seal failure temperature is quite apparent for seals made of both elastomers. However, the effect of roughness at relatively low ($\delta = 7-10\,\%$) seal compression ratios is not as significant as at high ($\delta = 25-30\,\%$) compression ratios. The plausible reason is related to the strength of adhesion between HNBR and the steel counter-face and will be discussed in the next section.

The second set of experiments was carried out using the rig with the sealing force measurement capability. Low temperatures have a profound effect on the retention of the sealing force of the tested O-rings as depicted in Fig. 6a. The O-ring sealing force decays with cooling to nearly zero at a variable decay rate which reaches a maximum at about $-10\,^{\circ}\mathrm{C}$. A similar behaviour of force decline during cooling at low temperatures was noticed earlier in fluoroelastomer [5, 7, 6] and HNBR [22, 14] seals. In addition, experiments were carried out on CB filled O-rings, and the effect of filler on the sealing force is quite apparent here. A higher amount of carbon black makes the retention of the sealing force at low temperatures better. This positive effect of the filler is in a good agreement with the results of the flange-

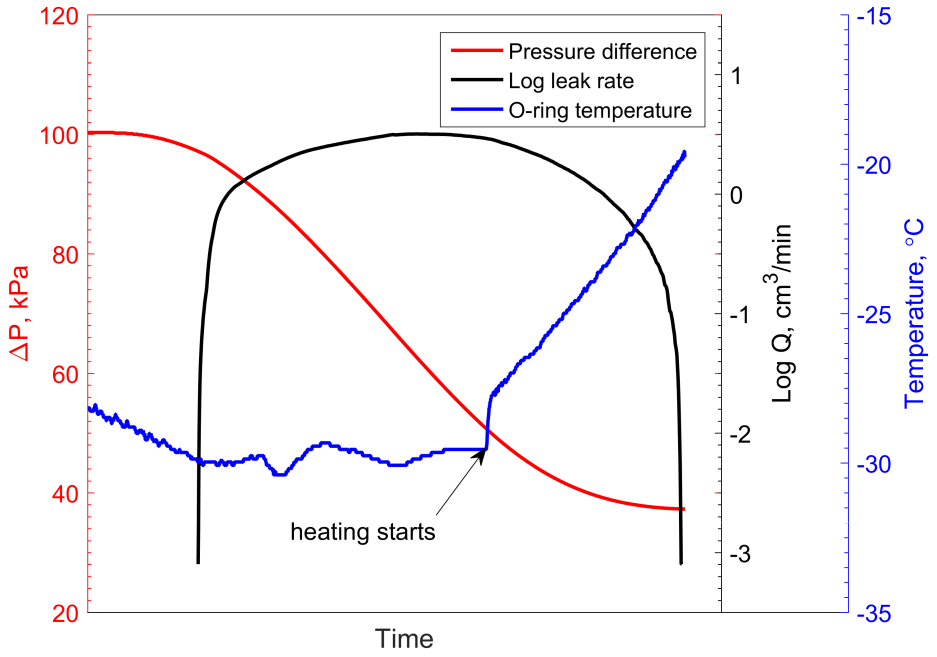

Figure 3: Pressure difference in the system, leak rate and temperature of an unfilled HNBR O-ring subjected to ≈ 8 % compression as function of time (grinding surface finish).

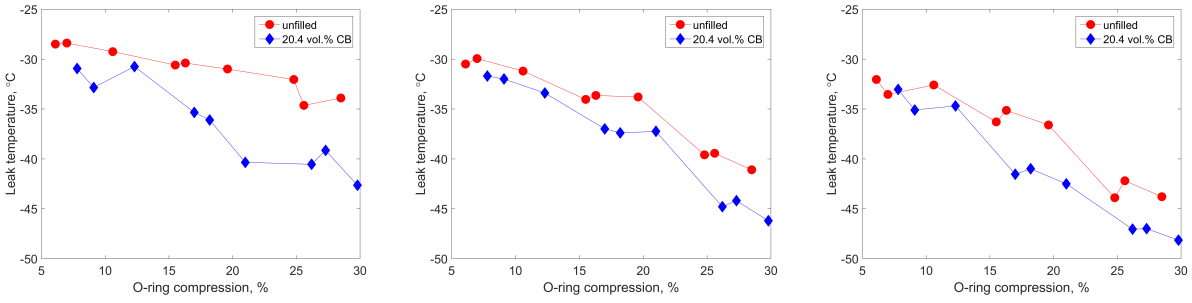

(a) Milling (b) Grinding (c) Turning

Figure 4: Leak temperature as function of seal compression for 20.4 vol.% CB filled and unfilled HNBR seals.

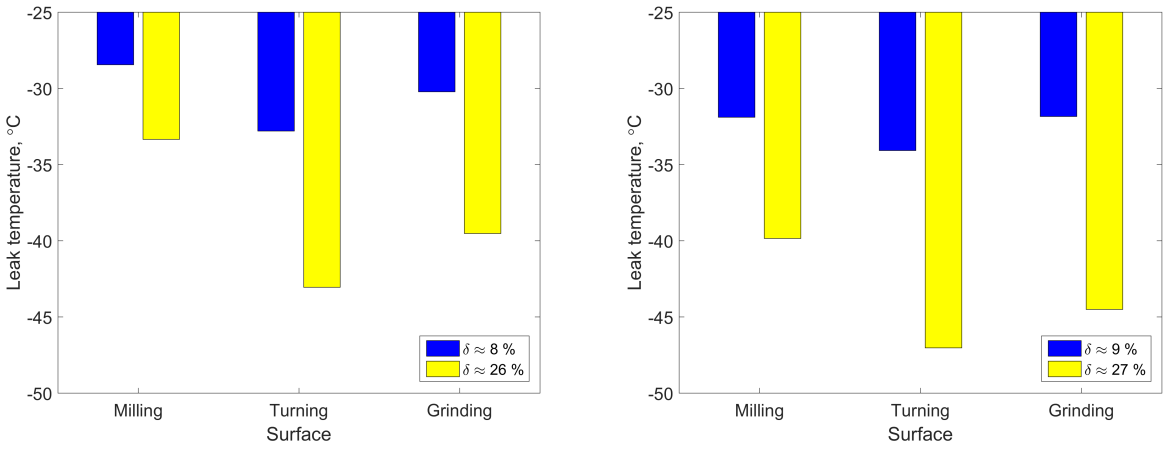

(a) unfilled HNBR

(b) 20.4 vol.% CB filled HNBR

Figure 5: The effect of surface finish on leak temperature a) in unfilled HNBR and b) in filled HNBR seals at the indicated seal compression ratio δ.

based leak experiments and attributed to a lower thermal contraction of the filled elastomers [19] as well as a lower contribution of the entropy elasticity [21]; see also the analysis and discussion below.

Another interesting phenomenon, which was not discovered in the earlier studies, is the abrupt force increase observed in our experiments at temperatures below the glass transition (see Fig. 6a). These force jumps led, in turn, to an drastic increase of the leak rates in every experiment, except for the seals lubricated by a silicone grease. This peculiar effect is believed to be related to breakage of the adhesive bond between the elastomer and its metal substrates at low temperatures as the thermal stresses in the rubber near the interface reach a critical value due to the thermal shrinkage [23]. The effect of adhesion on the cold leakage of O-rings will be discussed below. The abrupt increase in force at the moment of detachment is presumably caused by the O-ring sliding movement in radial direction due to its thermal shrinkage, see also Fig. 12 in the analysis part.

No significant increase of the leak rates was observed in grease lubricated seals, even though the seals detached from the counter-surface manifested in similar force jumps as in the dry O-rings, see Fig. 6b. The silicone grease is likely to fill up the gap formed at low temperatures between the HNBR seal and its counter-surface and, thereby, prevents the air flow through the gap.

4. Analysis and discussion

Leakage experiments of HNBR seals exposed to low temperatures at various compression levels were carried out using sealing surfaces with different topography. In order to understand the effects of compression and the counter-surface topography on leakage, a multi-scale approach to the contact mechanics of an elastomer seal ring against a rough rigid substrate has be to undertaken.

Consider a case of an O-ring seal squeezed between flange parts in a tight joint. The seal delimits a high and low pressure regions with the pressure drop ΔP. The nominal contact area A_0 between the O-ring and the rigid counter surface is $L_y \times L_x$ or $\pi D \times 2a$, where D is the seal diameter and a is the half-width of the contact region in the fluid leakage direction. It is well known [24], that most surfaces in engineering applications exhibit surface roughness on a wide range of length scales, which has to be accounted for in the contact studies. As such the contact area, for example, when observed with micro-scale resolution, will be smaller than the nominal one. This is due to the existence of microscopic peaks and valleys in the topography of the surface, even if the looks smooth and flat to the naked eye.

In order to quantify the effect of roughness on different levels mathematically, magnification ζ is introduced according to the Perssons contact theory [25]. The apparent contact area $A(\zeta)$ can be then studied as a function of

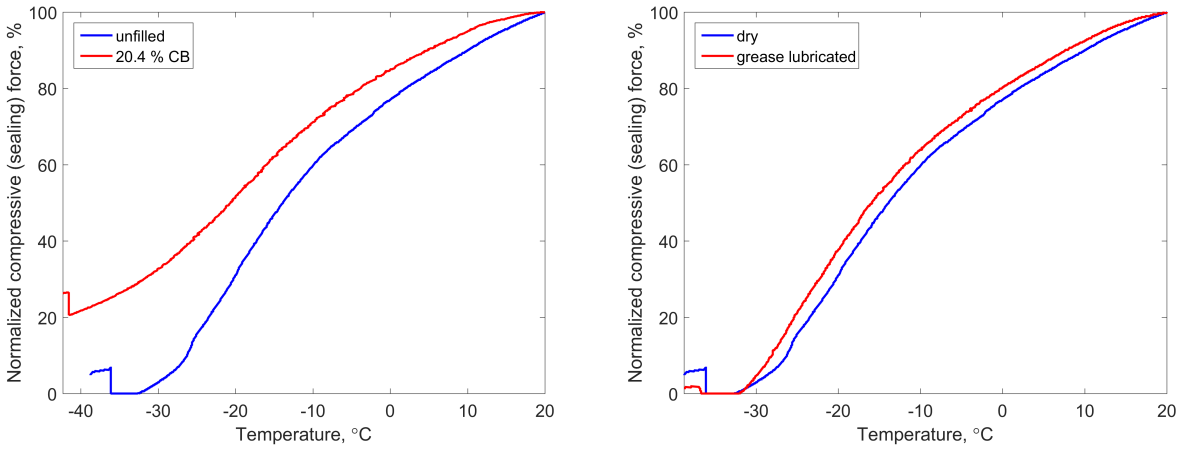

Figure 6: The effect of CB loading in a) and grease lubrication in b) on the temperature variation of the O-ring compressive force normalised to the compressive force at room temperature. The seals were compressed ($\delta = 0.1 \pm 0.005$) and left to relax under the constant strain for approximately 16-17 hours before the cooling step in order to minimise the effect of stress relaxation during the experiment.

magnification ζ. The contact between a rubber block and a rigid surface appears to be complete $A(1) = A_0$ at the lowest magnification $\zeta = 1$. At higher magnifications surface roughness can be observed and, thus, the apparent contact area decreases ($A(\zeta) < A_0$). The apparent relative contact area $A(\zeta)/A_0$ at the magnification ζ can be obtained using the Perssons contact theory [25, 24, 26] via

$$\frac{A(\zeta)}{A_0} = \text{erf}\left(\frac{P_0}{2G^{\frac{1}{2}}}\right) \tag{1}$$

where erf(x) is the error function, P_0 is the nominal contact pressure and the function G is expressed as

$$G(\zeta) = \frac{\pi}{4}\left(\frac{E}{1-\nu^2}\right)\int_{q_L}^{\zeta q_L} \mathrm{d}q q^3 C(q) \tag{2}$$

where $C(q)$ is the 2D surface roughness power spectrum, E and ν are the elastomer Youngs modulus and the Poissons ratio, $q = \zeta q_L$ (with $q = 2\pi/\lambda$ and $q_L = 2\pi/L_x$) is the wave vector and λ is the wavelength.

Estimation of the interfacial leak rate through a seal-rigid substrate contact can be done using the critical junction [28, 27] or effective medium theories [29, 30]. The latter is used here since it takes into account the leakage through multiple channels, not only the critical constriction channel as in the former approach. The effective medium theory treats a multi-component medium (e.g. a porous medium in the fluid flow studies) as a single phase medium with effective (averaged) properties. Assuming incompressible and laminar flow, the leak rate is calculated using the effective conductivity of the contact interface σ_{eff} in accordance with [29, 30]

$$Q = \frac{L_y}{L_x}\sigma_{\text{eff}}\Delta P \tag{3}$$

where

$$\frac{1}{\sigma_{\text{eff}}} = \int_1^{\zeta}\left(-\frac{A'(\zeta)}{A_0}\right)\frac{2}{\sigma_{\text{eff}} + \sigma(\zeta)}\mathrm{d}\zeta \tag{4}$$

and

$$\sigma(\zeta) = \frac{[u_1(\zeta)]^3}{12\mu} \tag{5}$$

Here $u_1(\zeta)$ is a function dependent on the average effective separation, μ is the sealed fluid viscosity. For more details on the theoretical foundation of the leak rate calculations, the reader is referred to the original publications [29, 30].

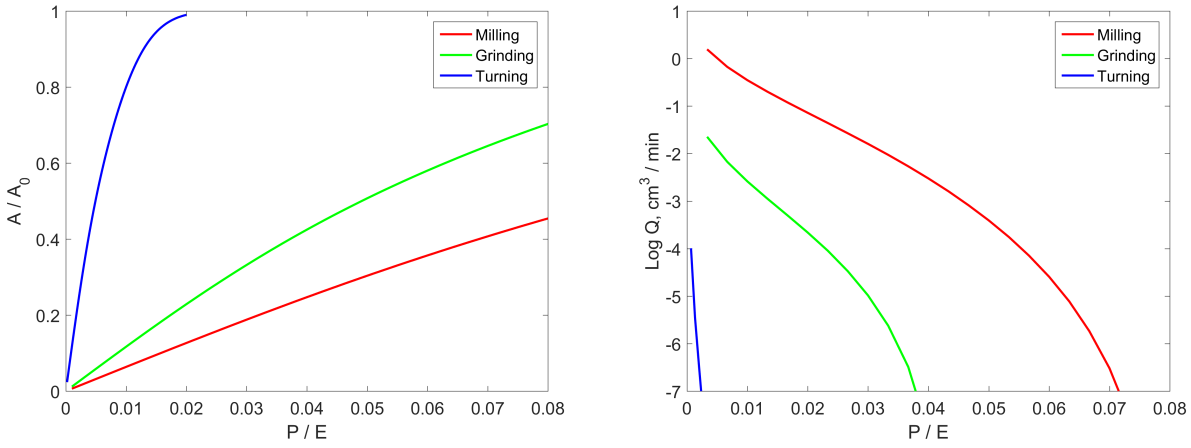

(a) (b)

Figure 7: Calculated relative contact area in a) and calculated leak rate Q in b) as functions of the normalized contact pressure at the indicated surface finish. The results were obtained using 1D power spectra depicted in Fig 2b without taking the adhesion and the surface roughness anisotropy into account.

The leak rates for the cases studied here were calculated using the methodology presented above. Fig. 7b depicts the outcome of leakage calculations with leak rate Q plotted against the normalized contact pressure (P_0/E). The surfaces evidently have different interfacial leakage characteristics. As expected, the milled surface represents the worst leakage case, while the surface produced by turning is characterized by the lowest leak rates. In fact, the real contact area (see Fig. 7a) reaches the percolation threshold (for $A(\zeta)/A_0 \approx 0.42$) at much lower compression than in the other cases which leads to an abrupt decrease of leak rate already at very small contact pressures ($P_0/E \geq 0.005$ or, for instance, $P_0 \geq 0.025$ MPa for the unfilled HNBR). In contrast, the contact pressure required to attain the percolation threshold for the surface after milling is about 16 times higher: $P_0/E \approx 0.08$ or $P_0 \approx 0.4$ MPa for the unfilled HNBR. This will have an effect on the leakage at low temperatures in addition to the other effects. It is noteworthy that the leak rates in Fig. 7b have to be multiplied by a factor of ≈ 1000 coming from the ratio L_y/L_x and even higher as the contact width L_x dramatically reduces with cooling, see the analysis of the contact below. In this study, the roughness of the HNBR O-ring surface is assumed smaller than the counter-surface roughness.

It is quite clear that the seal contact pressure is a very important characteristic for the leak rate in ambient conditions. Changes in the contact pressure with temperature is also likely to define the onset of the observed air breakthrough at temperatures below T_g. In order to understand the development of the contact pressure profile across the sealed interface with temperature, a finite element analysis (FEA) approach is utilized. An axisymmetric model of an O-ring with a cross section diameter of 5.5 mm was built and analysed using Abaqus software (v. 6.14). The model mesh was generated using the free meshing technique with quad-dominated elements [31]. CAX4RH linear hybrid elements with an average element size of 0.1 mm were utilized. Compression of the ring was done by rigid analytical surfaces.

The thermo-mechanical properties of the materials employed were obtained in the previous studies [19, 20, 21]. The thermal dilatation curves of the studied elastomers are depicted in Fig. 8a and implemented into the analysis as temperature dependent functions of the coefficients of thermal expansion, see Appendix A. It is worth mentioning that the CB filled HNBR apparently has a lower thermal expansivity than the unfilled material, i.e. $\alpha = 131 \times 10^{-6}\,1/°C$ for the CB filled HNBR vs $\alpha = 187 \times 10^{-6}\,1/°C$ for the unfilled compound (both values are given for the rubbery state).

The model takes into account long-term hyperelastic and viscoelastic (time-dependent) responses and finite com-

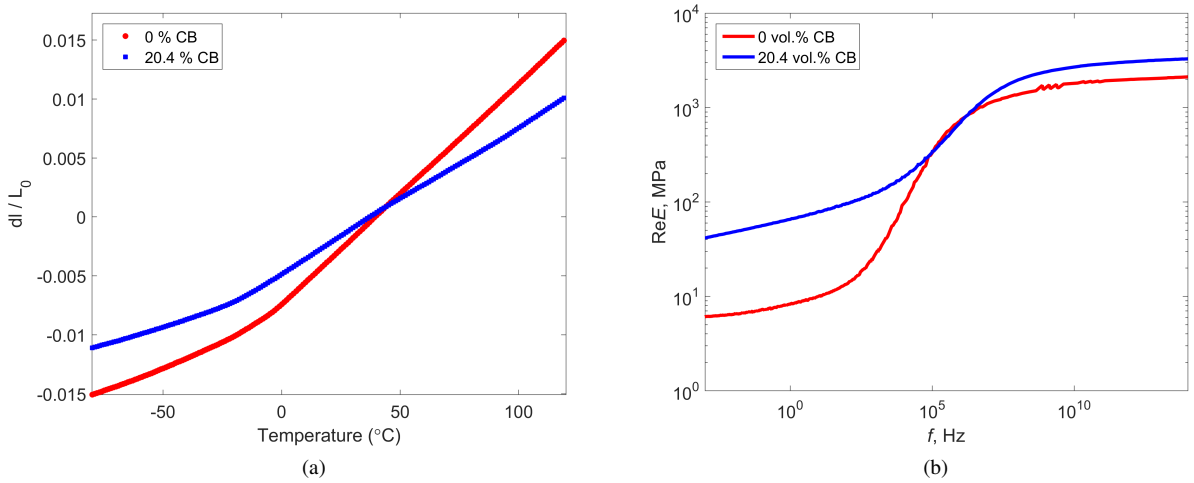

Figure 8: The thermo-mechanical data of HNBR at the indicated CB volume fraction: a) dilatometric curves and b) storage modulus master curves. The dilatometric measurements were carried out using Netzsch DIL402C dilatometer at a heating rate of 2 °C/min [19]. The dynamic tests were performed in tension using a TA instruments DMTA apparatus with a strain amplitude of 0.04 %. The frequency scan was made over a wide range of temperatures from -70 to 120 °C with a temperature increment of 5 °C (2.5 °C in the region from -30 to 30 °C) at 10 frequencies.

pressibility of the materials [19, 20]. Modelling the viscoelastic behaviour of the HNBR near the glass transition is not straightforward as it also exhibits an increasing strain dependency at about -15 °C and deeper into the glass transition [21]. However, considering the initial large-strain field in the seal is essentially frozen-in below the T_g [12, 20, 23], the modelling approach in the first approximation can be considerably simplified focusing only on the thermal shrinkage in the transition and glassy regions which causes small strain changes with each temperature increment ($\approx 0.1-0.2$ % over the total temperature range from -20 °C to -40 °C). Therefore, only small-strain viscoelastic material data are needed to get the corresponding Maxwell model parameters. The material data were collected by dynamic measurements in the linear range of HNBR. The data were then used to build storage modulus master curves depicted in Fig. 8b and compute the viscoelastic parameters to feed the viscoelastic part of the model. All material properties used in the simulation are listed in Appendix A.

An example of the FEA simulation is given in Fig. 9a-9c. The simulated contact pressure steadily decreases with cooling and, at temperatures below the glass transition, abruptly drops to zero. For the counter-surface produced by grinding, microscopic separation of the seal from the counter-part is likely to occur as the maximum contact pressure quickly falls below ≈ 0.25 MPa (or ≈ 0.51 MPa for the 20.4 vol.% CB filled compound). This in turn results in a drastic increase in the air leak rate through the contact. This contact pressure corresponds to the leak rate Q $\approx 10^{-3}$ cm^3/min estimated by the effective medium leakage theory for this surface (see Fig. 7b).

The simulation results are influenced by non-material parameters. The rate of cooling has a large impact on the cold seal failures as demonstrated by Fig. 10a built based on FEA simulation with various cooling rates. It is evident that the leakage temperature greatly increases at higher rates of cooling. The seal detaches from its substrate at temperatures above the T_g when the cooling rate of 1 °C/s is applied. It can be understood qualitatively as follows. As the rate of cooling grows, the ability of HNBR to recover and compensate for the thermal shrinkage becomes more and more inhibited. The elastic recovery in elastomers is a time (and temperature) dependent process [20] and the time window required for the seal to recover the thermal contraction becomes smaller and smaller with cooling in the transition and glassy regions. Therefore, the condition for the seal failure would be:

$$\dot{\varepsilon}_r \lessapprox \alpha(T)\dot{T} \tag{6}$$

where ε_r is the recoverable strain. The results of the FEA simulation also depend on the coefficient of friction (CoF) used as demonstrated in Fig. 10b. However, the sensitivity to the variation of CoF is not as substantial as the sensitivity to the cooling rate. Furthermore, a rather high friction is to be expected due to the adhesion and "locking" of the frozen

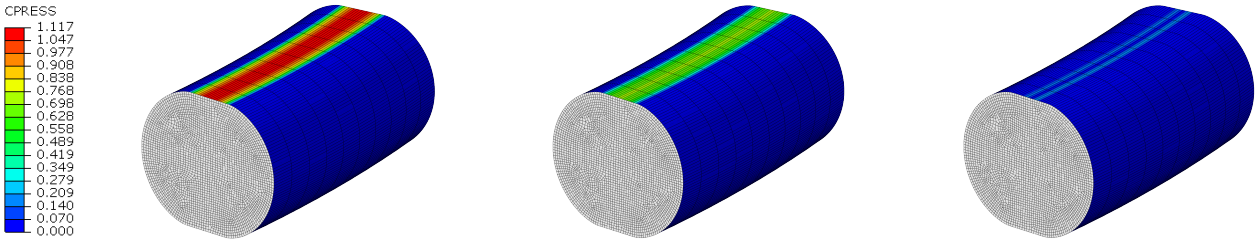

(a) T = 297 K (b) T = 253 K (c) T = 243 K

Figure 9: An example of the simulated contact pressure profile along the contact line of an O-ring section subjected to 10 % compression at ambient temperature and cooled down. The contact pressure scale bar is in MPa. The maximum contact pressure at −20 °C (253 K) is about a half of the initial one due to the thermal shrinkage of the HNBR and softening related to the entropic nature of the material. The contact pressure at −20 °C is still sufficient to retain the air tightness at 1 bar pressure difference (see Fig. 9b), whereas at −30 °C (243 K) it diminishes to nearly zero with a minor contact width resulting in leakage. The FEA was performed using a cooling rate of −0.01 °C/s and CoF of 0.5.

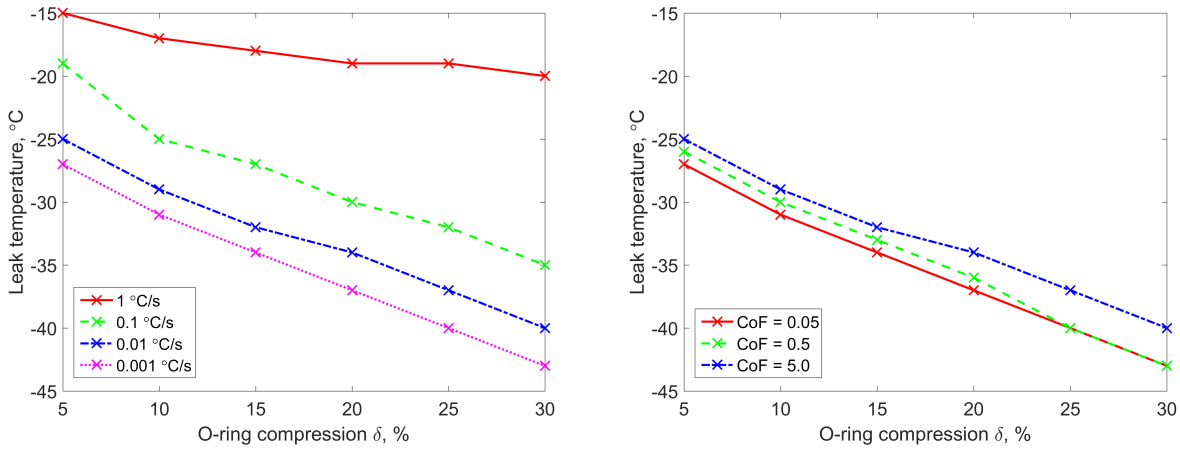

(a) (b)

Figure 10: The effects of cooling rate with CoF = 5 in a) and the coefficient of friction using the cooling rate of −0.01 °C/s in b) on the simulated seal failure temperatures for the unfilled HNBR compound.

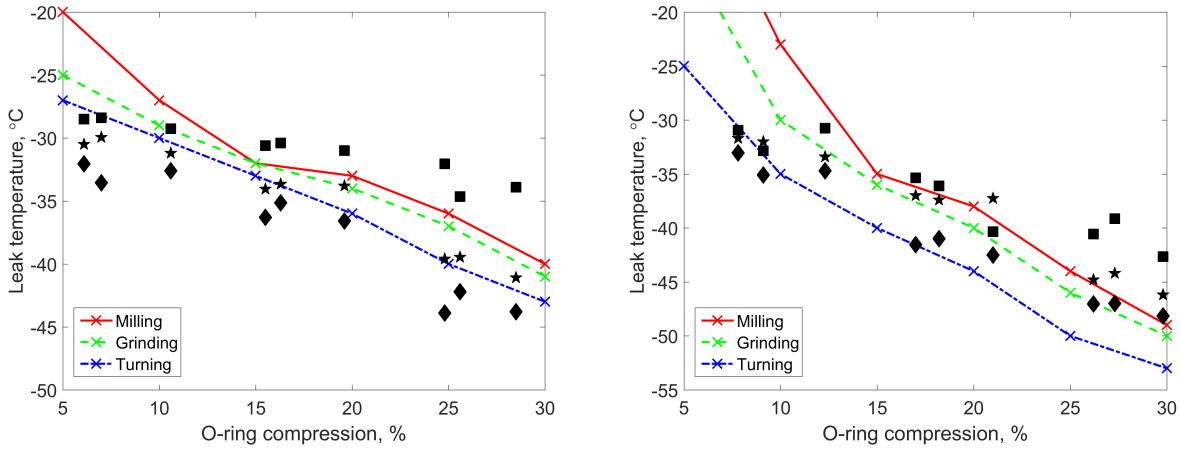

(a) Unfilled HNBR (b) 20.4 vol.% CB HNBR

Figure 11: Simulated and experimental leak temperatures as functions of seal initial compression for sealing surfaces with indicated surface treatment. The experimental data are for surfaces after milling (■), grinding (★) and turning (⧫) listed in the direction of roughness decrease. The FEA was performed using a cooling rate of −0.01 °C/s attained in the flange-based leak tests and CoF = 5.0.

elastomer between the steel asperities, especially in the roughest sealing surface.

The actual cooling rate of −0.01 °C/s achieved in the flange experiments is used in further analysis and comparison with the experimental leak data. The predicted seal failure temperature is plotted against the initial compression of the seal together with the experimental leak data for the 2 studied compounds in Fig. 11a and in Fig. 11b. The simplified FEA model is seen to capture the onset of air leakage in HNBR seals against the surface after grinding at temperatures below the T_g quite well, considering the data scatter and the assumptions used in the modelling approach. The difference between experimental and predicted leakage temperatures can also be attributed to quality of the data fitting with 13 Prony elements (maximum in Abaqus) and also cold adhesion phenomena.

It has been found above and in [23] that the adhesion bond between HNBR seal and its steel substrate might break at low temperatures due to thermal stresses in elastomer at the interface leading to the premature onset of air leakage. The adhesion of the HNBR O-ring compressed at ambient temperature to a rigid substrate is rather small (the pull-off force per unit length $f_{adh} \approx 0.04$ N/mm) at this temperature, however it is found to grow with cooling [23]. The effect is strongest for smooth and clean surfaces, whereas contaminated or rough surface might reduce the adhesion significantly. This difference can reach one order of magnitude (e.g. $f_{adh} \approx 0.2$ N/mm for roughened HNBR vs $f_{adh} \approx 1$ N/mm for clean and smooth HNBR [23]). The thermal stresses are generated in the elastomer rings due to thermal contraction both in radial and circumferential directions (the O-ring cross section and the circumference decrease with cooling). As soon as the normal or shear stresses exceed the adhesion strength at a critical temperature T_{crit}, the detachment of a glassy elastomer takes place. In turn, a large leakage might immediately develop since the deformation field in the elastomer seal is frozen-in in the initial compressed state (i.e. it has a negligible elastic recovery), as schematically illustrated in Fig. 12. The leak will be sustained if the seal is not able to recover within the experiment time, as most likely the case for with our leakage tests below T_g. Only external heating can help the elastomer to recover and close up the gap between the HNBR seal and its counter-surface.

A quantitative estimation of the thermal stresses in the direction orthogonal to the contact area and its effect on adhesion-connected seal failure temperatures can be made. The condition for the adhesion bond breakage is

$$S > S_{adh} \tag{7}$$

where the normal thermal stress $S = E\alpha\Delta T$ and the bond strength $S_{adh} = F_{adh}/(2aL_y) = f_{adh}/(2a)$. Hence, the temperature interval that the adhesion bond in glassy elastomer can sustain without failure (assuming no recovery) is

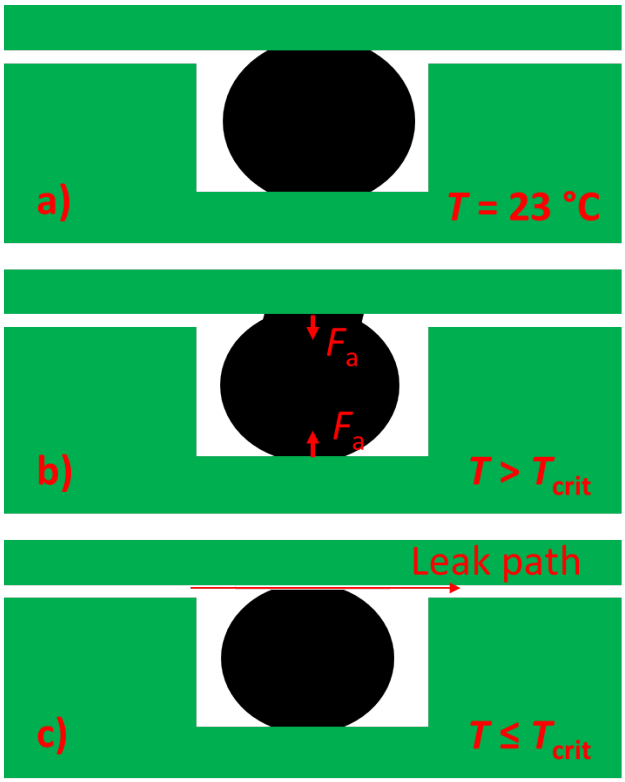

Figure 12: Schematic of the O-ring compressed in a flange joint a) at room temperature, b) cooled down to a low temperature (rubber-steel adhesion increases with cooling down to T_g), c) cooled down to the critical temperature ($T_{crit} < T_g$) at which debonding and subsequent leakage occur.

$$\Delta T_{\mathrm{adh}} = \frac{f_{\mathrm{adh}}}{2aE\alpha} \tag{8}$$

Consider two limiting cases of weak and strong cold adhesion measured using unfilled HNBR O-ring sections [23], i.e. the pull-off force per unit length of O-ring of 0.2 N/mm and 1 N/mm respectively in the case of 10 % initial compression. Thus, using the glassy modulus E of 2 GPa and $\alpha \approx 8 \times 10^{-5}\,^{\circ}\mathrm{C}^{-1}$ the lower and upper bounds of ΔT_{adh} are $\approx 1.2\,^{\circ}\mathrm{C}$ and $\approx 6\,^{\circ}\mathrm{C}$. Since f_{adh} increases with $\sqrt{a}$ (or $\approx \delta^{1/4}$) [23] while the contact area linearly grows with a (or $\approx \sqrt{\delta}$), it can be concluded that the adhesion bond might fail earlier (at lower ΔT_{adh}) at higher compression ratios δ. The opposite is of course true at lower δ, e.g. 5 %. Similar observations can be made taking the elastic modulus (f_{adh} scales with $\sqrt{E}$ [23], while the thermal stress has a linear relationship with E). In general, more work is required to study the phenomenon of elastomer adhesion to various substrates at low temperatures and factors influencing it.

The results also signify the effect of the thermal contraction of static seal material at the point where the frozen seal cannot recover within the experimental time scale. The importance of the elastomer thermal contraction at and below T_{g} is much higher than estimated before [32]. It is clear that the CB filled HNBR seals with the coefficient of thermal expansion $\alpha \approx 6 \times 10^{-5}\,^{\circ}\mathrm{C}^{-1}$ in the glassy state yielded better cold leakage performance than the unfilled counterparts with $\alpha \approx 8 \times 10^{-5}\,^{\circ}\mathrm{C}^{-1}$, in spite of the inferior cold-recovery properties of the filled HNBR [20]. This is also supported by the experimental data of the sealing force decay which is significantly lower in CB filled HNBR seals. Therefore, having an elastomer with a small CTE (ideally $\leq 1 \times 10^{-5}\,^{\circ}\mathrm{C}^{-1}$ for contact with steel counter-parts) would be very beneficial for sealing applications where permanent or periodic exposure to temperatures reaching the glass transition and below it is foreseen.

5. Conclusions

Cold performance of static hydrogenated nitrile butadiene rubber (HNBR) O-ring seals subjected to various degrees of compression is studied using low (1 bar) pressure difference. When cooling down to temperatures below the glass transition point T_{g} of HNBR (−23 °C), an abrupt increase of air leakage ($> 10^{-2}\,\mathrm{cm}^3/\mathrm{min}$) is observed. The experimental results demonstrate that the seal failure temperatures are affected by surface finish conditions, variation of the compression ratio of the seals and additions of carbon black (CB) in the HNBR. The seal compression force is also found to decrease with cooling and the rate of the compression force decay depends on the CB content. In addition, an abrupt increase of compression force followed by a sudden increase of the leak rate in HNBR seals was observed at low temperatures $< T_{\mathrm{g}}$. This effect is believed to be caused by failure of the HNBR-substrate adhesion bond induced by thermal shrinkage of the elastomer. The origin and conditions of the cold adhesion and its failure is explained in our separate publication [23].

The main reason for the seal failures is believed to be detachment of the elastomer seals from their mating sealing parts due to a) breakage of the adhesion bond induced by the elastomer thermal contraction in case of a rather strong adhesion bond and negligible recovery of the HNBR below T_{g} or b) due to the thermal contraction and the negligible recovery when the strong adhesion bond is not formed. It is shown that most of the cold failures can be modelled by the effective medium leakage theory and a simple finite element analysis (FEA) approach using thermo-mechanical material data the most important of which are the thermal expansivity and small-strain viscoelasticity of HNBR. Despite the worse recovery properties, the CB filled HNBR has a lower thermal expansion which results in a better retention of the sealing force and lower leakage temperatures if compared to the seals made of the unfilled HNBR. Hence, it can be inferred that a better low-temperature serviceability in static joints can be achieved using elastomer compounds with low coefficients of thermal expansion ideally close to the one of the seal housing material.

No leakage was found in silicone grease lubricated seals which is likely to fill the gap between the HNBR and its counter-surface after the separation of HNBR seal from it in a cold environment. However, the effect of the grease and other industrial lubricants on cold adhesion is unclear and should be studied in more detail. Furthermore, the grease might squeeze out with time or might be washed away by service fluids, and, therefore, a different leakage behaviour should be expected in circumstances other than in this work.

6. Acknowledgement

This work was supported by the Research Council of Norway (Project 234115 in the Petromaks2 programme), FMC Kongsberg Subsea AS and STATOIL Petroleum AS, with the research partners Norwegian University of Science and Technology (NTNU) and SINTEF Materials and Chemistry. This work is also supported in part by EU COST Action MP1303. The authors would like to thank Dr. Peter Köllensperger and Ida Marie Eriksdatter Høiaas for the surface topography measurements at NTNU NanoLab and Boris Lorenz and Avinash Tiwari for DMTA measurements at FZ Jülich.

7. References

References

[1] Müller HK, Nau BS. Fluid sealing technology : principles and applications. New York: M. Dekker; 1998. 485 p.
[2] Baranov, NS, Sokolov VE, Elkin AI. Contact leaks through flange joints sealed by circular and square-section rubber seals (in Russian). Kauch. & Rezina 1982;8: 25-28.
[3] Alcock B, Peters TA, Gaarder RH, Jørgensen JK. The effect of hydrocarbon ageing on the mechanical properties, apparent crosslink density and CO2 diffusion of a hydrogenated nitrile butadiene rubber (HNBR).Polymer Testing 2015; 47: 22-29.
[4] Salita M. Simple finite-element model of o-ring deformation and activation during squeeze and pressurization. J Propul Power. 1988;4(6):497-511
[5] Stevens RD, Thomas EW, Brown JH, Revolta WNK. Low temperature sealing capabilities of fluoroelastomers. SAE Technical Papers. 1990.
[6] Burnay SG, Nelson K. Leakage of transport container seals during slow thermal cycling to -40-degrees-C. International Journal of Radioactive Materials Transport. 1991;2:91-6.
[7] Streit G, Achenbach M, Kanters A. Sealability of O-rings at low-temperatures .1. Sealability without media influence at low-temperatures. Kaut Gummi Kunstst. 1991;44(9):866-70.
[8] Taylor KW. Performance Characteristics of Oilfield Proven Elastomers in Low-Temperature Seal Applications. 23rd Annual Offshore Technology Conference; 1991/1/1/; Houston, Texas. OTC: Offshore Technology Conference; 1991. p. 193-206.
[9] Weise HP, Kowalewsky H, Wenz R. Behaviour of elastomeric seals at low temperature. Vacuum. 1992;43(5):555-7.
[10] Warren P. Low temperature sealing capability of elastomer O-rings. Sealing Technology. 2008;9:7-10.
[11] Jaunich M, von der Ehe K, Wolff D, Voelzke H, Stark W. Understanding low temperature properties of elastomer seals. Packaging, Transport, Storage & Security of Radioactive Material. 2011;22(2):83-8.
[12] Jaunich M. Tieftemperaturverhalten von Elastomeren im Dichtungseinsatz. PhD thesis, BAM-Dissertationsreihe Vol. 79. Berlin: Bundesanstalt für Materialforschung und Prüfung; 2012. 143 p.
[13] Grelle T, Wolff D, Jaunich M. Temperature-dependent leak tightness of elastomer seals after partial and rapid release of compression. Polymer Testing. 2015;48:44-9.
[14] Omnés B, Heuillet P. Leak tightness of elastomeric seal at low temperature: Experimental and fem-simulation. In:Constitutive Models for Rubber IX. ECCMR 2015: Proceedings of the 9th European Conference on Constitutive Models for Rubbers; 2015, p. 60914.
[15] Zhang B, Yu M, Yang HY. Leakage analysis and ground tests of the O-type rubber ring seal applied in lunar sample return devices. P I Mech Eng G-J Aer. 2015;229(3):479-91.
[16] Grelle T, Wolff D, Jaunich M. Leakage behaviour of elastomer seals under dynamic unloading conditions at low temperatures. Polymer Testing. 2017;58:219-26.
[17] Chen X, Bartos J, Salem H, Zonoz R. Elastomers for high pressure low temperature HPLT sealing. In: Offshore Technology Conference. OTC 2016: Proceedings of the Offshore Technology Conference; 2016, p. 382842.
[18] Drobny JG (Ed.). Fluoroelastomers Handbook. The Definitive User's Guide (Second Edition). William Andrew Publishing. 2016, 485 p.
[19] Akulichev AG, Alcock B, Tiwari A, Echtermeyer AT. Thermomechanical properties of zirconium tungstate/hydrogenated nitrile butadiene rubber (HNBR) composites for low-temperature applications. J Mater Sci. 2016;51(24):10714-26.
[20] Akulichev AG, Alcock B, Echtermeyer AT. Elastic recovery after compression in HNBR at low and moderate temperatures: Experiment and modelling. Polymer Testing. 2017;61:46-56.
[21] Akulichev AG, Alcock B, Echtermeyer AT. Stress relaxation in carbon black reinforced HNBR at low temperatures. Polymer Testing. 2017;63:226-35.
[22] Hornig R, Sunder J, Herr B. Static cold sealing force behaviour of amorphous HNBR materials. International Polymer Science and Technology. 2012;39:T1-T14.
[23] Akulichev AG, Tiwari A, Dorogin L, Echtermeyer AT, and Persson BNJ, *Rubber adhesion below the glass transition temperature: role of frozen-in elastic deformations* (submitted) (2017).
[24] Persson BNJ, Albohr O, Tartaglino U, Volokitin AI, Tosatti E. On the nature of surface roughness with application to contact mechanics, sealing, rubber friction and adhesion. Journal of Physics: Condensed Matter. 2005;17(1):R1.
[25] Persson BNJ. Theory of rubber friction and contact mechanics. J Chem Phys. 2001;115(8):3840-61.
[26] Yang C, Persson BNJ. Contact mechanics: contact area and interfacial separation from small contact to full contact. Journal of Physics: Condensed Matter.
[27] Persson BNJ, Yang C. Theory of the leak-rate of seals. Journal of Physics: Condensed Matter. 2008;20(31):315011.
[28] Bottiglione F, Carbone G, Mantriota G. Fluid leakage in seals: An approach based on percolation theory. Tribology International. 2009;42(5):731-7.

[29] Lorenz B, Persson BNJ. Leak rate of seals: Effective-medium theory and comparison with experiment. The European Physical Journal E. 2010;31(2):159-67.
[30] Persson BNJ. Fluid dynamics at the interface between contacting elastic solids with randomly rough surfaces. Journal of Physics: Condensed Matter 2010;22: 265004.
[31] Abaqus/CAE user's guide. Ver. 6.14. Providence, RI: Dassault Systémes; 2014.
[32] Shubin SN, Freidin AB, Akulichev AG. Elastomer composites based on filler with negative thermal expansion coefficient in sealing application. Archive of Applied Mechanics. 2016;86(1-2):351-60.

Appendix A. Material properties used in FEA

Appendix A.1. Thermal expansion

Thermal expansion properties

T, °C	α, 1/°C	
	0 vol.% CB	20.4 vol.% CB
-50	0.000131	0.000104
-40	0.000141	0.000112
-30	0.000153	0.000119
-20	0.000167	0.000126
-10	0.00018	0.000129
0	0.000188	0.000131

Appendix A.2. Hyperelastic model parameters

Hyperelastic material model parameters

T, °C	C_{10}, MPa		D_1, MPa^{-1}	
	0 vol.% CB	20.4 vol.% CB	0 vol.% CB	20.4 vol.% CB
-20	0.715	1.595	0.001	0.00087
-10	0.754	1.644	0.001	0.00087
10	0.816	1.743	0.001	0.00087
23	0.863	1.807	0.001	0.00087

Appendix A.3. Viscolastic model parameters

Viscolastic material model parameters

0 vol.% CB		20.4 vol.% CB	
g_i	τ_i	g_i	τ_i
0.016446	3.88E-11	0.0091265	8.13E-15
0.084958	4.05E-10	0.077912	1.90E-13
0.12617	4.23E-09	0.10678	4.44E-12
0.18243	4.42E-08	0.17927	1.04E-10
0.24471	4.62E-07	0.27004	2.42E-09
0.24072	4.82E-06	0.21934	5.66E-08
0.080891	5.04E-05	0.073866	1.32E-06
0.013841	0.00052604	0.02312	3.09E-05
0.003442	0.0054945	0.0095157	0.00072235
0.0010951	0.05739	0.0059176	0.016879
0.00094397	0.59944	0.0046534	0.39441
0.00035235	6.2612	0.0030326	9.2161
0.00058876	65.398	0.011327	215.35

Appendix A.4. Time temperature superposition (WLF) parameters

TTS parameters

Material	T_{ref}	C_1	C_2
0 vol.% CB	293	4.3661	71.1068
20.4 vol.% CB	293	8.41	91.0144